A water-soluble Manganese complex for selective electrocatalytic CO_2 reduction to CO

James J. Walsh,[a,b]† Gaia Neri[c] † Charlotte L. Smith[c] and Alexander J. Cowan[c] *

AUTHOR ADDRESS:

[a] School of Chemical Sciences, Dublin City University, Glasnevin, Dublin 9, Ireland

[b] National Centre for Sensor Research, Dublin City University, Glasnevin, Dublin 9, Ireland

[c] Department of Chemistry, Stephenson Institute for Renewable Energy, The University of Liverpool, UK.

Supporting Information Placeholder

ABSTRACT: Relatively few solution electrocatalysts for CO_2 reduction in aqueous solutions are reported. However to be sustainable, electrocatalytic CO_2 reduction is likely to be coupled to water oxidation in a complete device. Here we report a water soluble Mn polypyridyl complex for the electrocatalytic reduction of CO_2 to CO. This complex shows activity across a broad pH range and an excellent selectivity at pH 9 (3.8:1, CO:H_2). Cyclic voltammetry indicates activity across a range of different electrode materials (Boron doped diamond, glassy carbon and Hg/Au amalgams).

INTRODUCTION

Rising atmospheric CO_2 levels are a critical challenge facing society. An attractive option is to electrocatalytically[1] or photocatalytically[2] reduce CO_2 to fuels or feedstocks. The direct electrocatalytic one-electron reduction of CO_2 is thermodynamically challenging; however, the energy required is considerably reduced by directing catalysis *via* proton-coupled reduction pathways (e.g. $CO_2 + 2e^- + 2H^+ \rightarrow CO + H_2O$, E^0 = -0.73 V *vs.* Ag/AgCl at pH 7).[3] A serious complication is the competitive hydrogen evolution reaction which occurs at a similar potential ($2H^+ + 2e^- \rightarrow H_2$, E^0 = -0.61 V *vs.* Ag/AgCl at pH 7), making it necessary to develop catalysts with high levels of selectivity for CO_2 reduction.

Many homogeneous molecular catalysts which are selective for CO_2 reduction are known[4] although catalysis is often reported in organic solvents such as acetonitrile (CH_3CN) or *N*,*N*-dimethylformamide (DMF) with an additional proton source added in a low concentration (typically 5%). However, to enable a practical electrolyser that reduces CO_2 using water as the electron source, the ability to operate in aqueous solutions is desired. The increased proton concentration in aqueous solvents accentuates the need for selectivity and relatively few water-soluble molecular electrocatalysts for selective CO_2 reduction are known. Some examples include an iron(III) tetraphenylporphyrin functionalised with trimethylammonium groups which reduces CO_2 selectively at pH 6.7;[5] $[Ni(cyclam)]^{2+}$ [6, 7] and its derivatives (where cyclam = 1,4,8,11-tetraazacyclotetradecane);[8, 9, 10, 11] an Ir-pincer complex;[12] and, the recently reported [Re(4,4′-hydroxymethyl-2,2′-bipyridine)$(CO)_3$Br].[13]

Mn complexes of the form [Mn(bpy)$(CO)_3$Br] (where bpy = 2,2′-bipyridyl) were first reported to be active for CO_2 reduction to CO in CH_3CN/H_2O (95:5) in 2011.[14] Since then numerous studies of this class of electrocatalysts have been reported due their ability to reduce CO_2 at moderate overpotentials and use of abundant elements.[15–20] Spectroelectrochemical studies[21–24] have shown that [Mn(bpy)$(CO)_3$Br] is not the active catalytic species, instead formation of the primary active catalyst occurs *via* a one-electron reduction and bromide ligand loss to yield the dimer 1/2[Mn_2(bpy)$_2(CO)_6$], followed by a subsequent one-electron reduction to yield the five co-ordinate active catalyst $[Mn(bpy)(CO)_3]^-$. For some derivatives (e.g. [Mn(bpy(Me)$_2$)$(CO)_3$Br], where (bpy(Me)$_2$) = 4,4'-dimethyl-2,2'-bipyridine), CO_2 reduction has also been reported to occur *via* direct addition of CO_2 and H^+ to the initially formed dimeric species,[25] although in most cases the primary catalytically active species is instead $[Mn(bpy)(CO)_3]^-$.

A common feature of the studies of these Mn catalysts in solution to date has been the use of organic solvents which, in addition to conferring solubility, can contribute to suppressing competitive H_2 evolution. However, there is increasing evidence of the highly selective nature of this class of complexes towards CO_2 reduction making their study in water of interest. In previous reports we[26, 27] made use of the lack of aqueous solubility of [Mn(bpy)$(CO)_3$Br] to immobilise the complex within a Nafion film on a multi-wall carbon nanotube/glassy carbon (MWCNT/GC) electrode for heterogeneous CO_2 reduction in water. These first reports of heterogenized systems achieved relatively high current densities (> 4 m A cm^{-2}), stable activity (turnover numbers (TON) > 470) and selectivities of up to ~2:1 CO:H_2; however, they also required relatively high overpotentials (typically η = 0.48 to 0.83 V) to operate. More recently, a pyrene-modified [Mn(bpy)$(CO)_3$Br] derivative was also immobilised on MWCNT and was reported to operate in water at η = 0.55 and TON_{CO} > 1000, with a mixture of H_2, CO and formate being produced depending on the catalyst surface loading.[28]

Very recently a polymerised Mn complex also showed catalytic activity in water.[29] It is therefore important that this class of catalysts is further studied in aqueous electrolytes; however, to the best of our knowledge, the homogeneous electrocatalytic reduction of CO_2 in aqueous solvents has not been previously reported.

Here we report the electrocatalytic behaviour of $[Mn^I(bpy(COOH)_2)(CO)_3Br]$ (where $(bpy(COOH)_2)$ = 4,4'-dicarboxy-2,2'-bipyridine) in water. In a past study we attempted to modify the operating potential of this class of Mn carbonyl catalysts through modification of the bpy ligand in the 4,4' position.[27] Although the addition of electron withdrawing carboxylic acid groups did shift the first and second reduction potentials of the complex in CH_3CN positively with respect to the unmodified bpy complex, the catalytic activity in acetonitrile/water (95:5) electrolyte was modest when compared to the parent $[Mn(bpy)(CO)_3Br]$. However, here we show that the presence of the carboxylate groups imparts aqueous solubility, and in water $[Mn^I(bpy(COOH)_2)(CO)_3Br]$ shows a high level of selectivity towards CO_2 reduction.

RESULTS AND DISCUSSION

$[Mn^I(bpy(COOH)_2)(CO)_3Br]$ is soluble to concentrations of *ca*. 0.5 mM (Figs. S1, S2) when dissolved in pure water, with a 0.5 mM solution having pH 3.5 in air. Using Britton-Robinson buffer at higher pH (9.7) the solubility is increased, and solutions up to 5 mM can be achieved (Figs. S1, S2). To explore the pH-dependent behavior of this complex, UV/Vis spectra of $[Mn(bpy(COOH)_2)(CO)_3Br]$ between pH 1.5 – 12.5 have been recorded. At pH 3.5 the UV/Vis spectrum is typical of complexes of this type, with a MLCT absorption at 410 nm (blue-shifted relative to in CH_3CN, λ_{max} = 460 nm, Fig. S3), and a π-π^* transition at 300 nm, Fig. 1(a, c). The large shift in MLCT maxima is primarily due to ligand exchange, Fig. S4. As shown below in aqueous solution the bromide is displaced by water.

Both the MLCT and the π-π^* bands show a pH dependence at high (10-12.5) and low (1.5-3.5) pH values, Fig. 1. A titration in the mid-pH range showed no spectral changes. The spectral dependence at low pH values is assigned to the carboxylic acid groups on the bipyridine ligand, $[Mn^I(bpy(COOH)_2)(CO)_3(OH_2)]^+$ to $2H^+$ + $[Mn^I(bpy(COO)_2)(CO)_3(OH_2)]^-$. Previous studies on related Re and Ru complexes with carboxylic acid-modified bpy ligands have shown two distinct pK_a values, one for each carboxylic acid group on the bpy ligand. Our data can be adequately fitted to either a single pK_a (2.52 ± 0.8) or two close-lying pK_a values (2.60 ± 0.06, 2.25 ± 0.10) suggesting similar behavior.[30, 31] The pK_a of 11.65 is attributed to deprotonation of the aquo complex, $[Mn^I(bpy(COO)_2)(CO)_3(OH_2)]^-$ that is formed following the displacement of Br^- in water. The formation of an aquo complex is confirmed through mass spectrometry (Fig. S5) and FTIR spectroscopy (Fig. S6). The measured pK_a is in-line with the analogous complexes $[Re(bpy(CH_2OH)_2)(CO)_3(OH_2)]^+$ and $[Re(bpy)(CO)_3(OH_2)]^+$.[13] In this past study addition of CO_2 caused precipitation of $[Re(bpy)(CO)_3(OC(O)OH)]$, whilst $[Re(bpy(CH_2OH)_2)(CO)_3(OC(O)OH)]^+$ remained soluble in CO_2 saturated water. Here we find that $[Mn^I(bpy(COO)_2)(CO)_3(OH_2)]^-$ remains soluble under CO_2. The UV/Vis spectra in the presence and absence of CO_2 are very similar, both in water and carbonate electrolyte, therefore our control experiment suggests that displacement of the aquo ligand by bicarbonate does not occur extensively and if formed the carbonato adduct is not the majority species, Fig. S7.

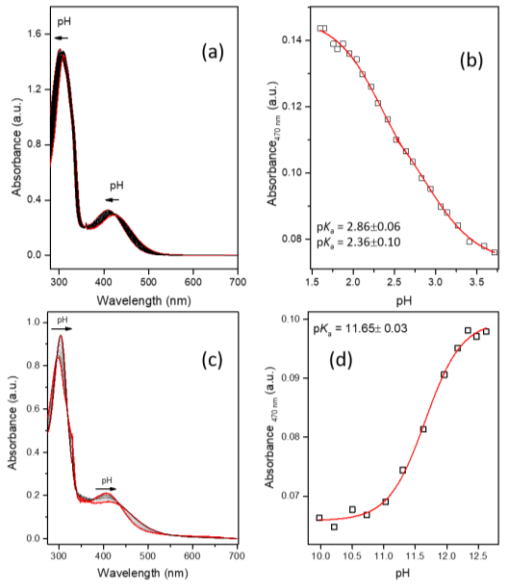

Fig. 1: UV/Vis spectra recorded following the preparation of solutions using $[Mn^I(bpy)(COOH)_2)(CO)_3Br]$ 8.6 x 10^{-5} M in Britton-Robinson buffer between pH 1.5-3.5 (a) and 10-12.5 (c). pK_a values were obtained from a plot of the absorbance at 470 nm versus the pH of the solution (b), (d).

To enable the study of the electrochemical behavior of this complex across a wide pH range we have initially used a Hg/Au amalgam working electrode, Fig. 2. Amalgam electrodes have a wide potential window in aqueous electrolyte, permitting the study of redox processes at negative potentials and low pH that would be unobservable with more commonly employed electrode materials (e.g. glassy carbon).[32] Between pH 11.5 and 4 the CVs of $[Mn^I(bpy(COO)_2)(CO)_3(OH_2)]^-$ show two irreversible reductions, at -1.04 (± 0.03) V and -1.35 (± 0.03) V whose positions are not strongly dependent upon the pH (accurate E_{red} at each pH are reported in Table S1), Fig. 2. UV/Vis spectroelectrochemical studies of $[Mn^I(bpy(COOH)_2)(CO)_3Br]$ in DMF show that in aprotic solvents this complex behaves similarly to related complexes,[27, 33] with the first reduction being assigned to the reduction of $[Mn^I(bpy(COO)_2)(CO)_3(DMF)]^-$ which can undergo loss of the solvent ligand and dimerization. The dimer is then reduced in a 2 electron process to form 2 equivalents of $[Mn^0(bpy(COO)_2)(CO)_3]^{3-}$, Fig. S8, Table S2. Spectroelectrochemical experiments in aqueous solvents are more challenging as gas evolution, even under Ar due to H_2 production, from the most commonly used mesh electrodes can prevent accurate optical transmission measurements. However at relatively high pH's (9) we have been able to study the first reduction of $[Mn^I(bpy(COO)_2)(CO)_3(OH_2)]^-$ at a carbon foam electrode, Fig 3. The UV/Vis data is shown as a difference spectrum. New positive bands indicate the formation of new species. At potentials negative of the first reduction (-1.3 V versus an Ag wire pseudo reference electrode) bands at 393, 536, 641 and 824 nm are observed. UV/Vis maxima around 800 nm are commonly observed with a range of binuclear Mn diimine complexes.[34] With the exception of the band at 536 nm, there is good agreement with the UV/Vis spectrum of the dimer complex in DMF (380, 499, 644 and 810 nm, Table S2).

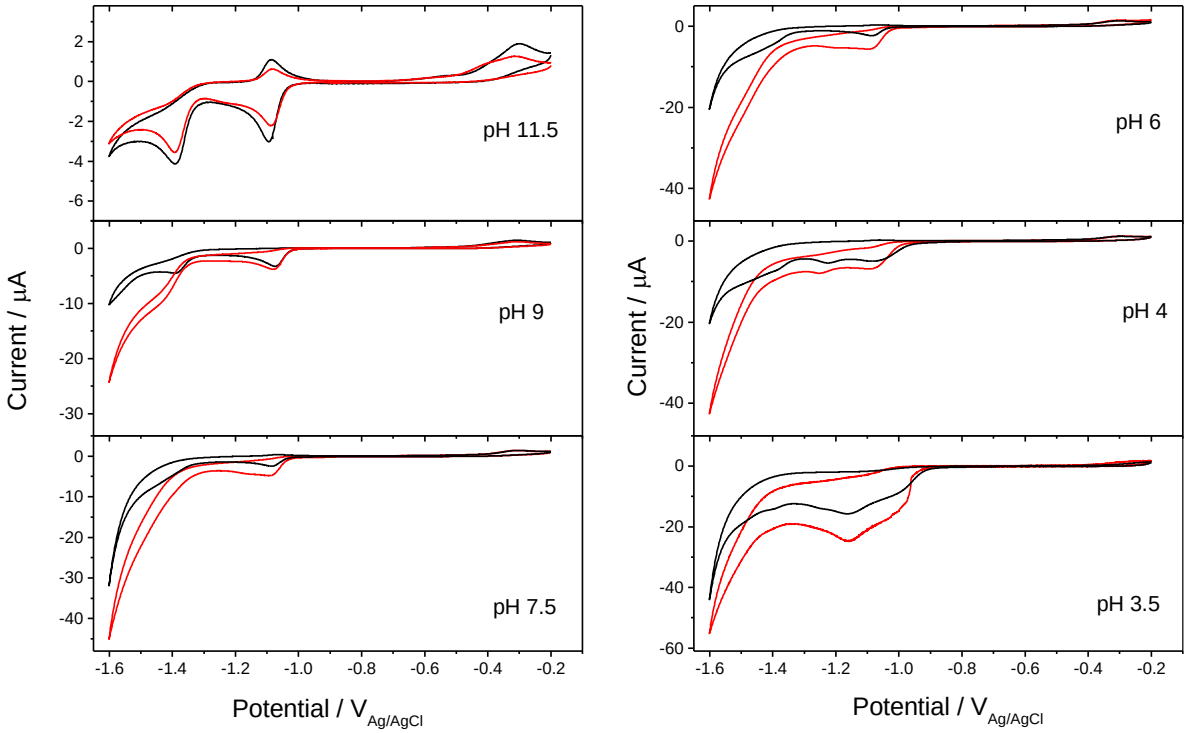

Fig. 2: CVs of [Mn(bpy)(CO$_2$H))(CO)$_3$(OH$_2$)]$^+$/[Mn(bpy)(COO)$_2$)(CO)$_3$(OH$_2$)]$^-$/[Mn(bpy)(COO)$_2$)(CO)$_3$(OH)]$^{2-}$ (0.5 mM total concentration), under argon (black) and CO$_2$ (red), carried out at a scan rate of 100 mV s^{-1}, Hg/Au WE. The electrolyte was K$_2$CO$_3$ (0.5 M) + KCl (0.1 M) for pH 11.5-7.5, 0.1 M KCl for pH 3.5-6 as prepared, and adjusted to the desired value by adding aliquots of either HCl or KOH solutions.

Therefore we assign the first reduction to the formation of [Mn(bpy(COO)$_2$)(CO)$_3$]$_2^{4-}$ which we anticipate can be reduced at the 2nd reduction to form the active catalyst, [Mn(bpy(COO)$_2$)(CO)$_3$]$^{3-}$. The UV/Vis band in figure 3 in water at 536 nm is currently unassigned. It may also arise from the dimer complex with the difference to the DMF spectrum being due to solvatochromism, however it is also feasible that additional species are present at potentials close to the first reduction and future spectroelectrochemical studies will explore this interesting behavior.

At potentials negative of -1.40 V when the pH ≤ 7.5 we observe a steep increase in current under argon suggesting that electrocatalytic hydrogen evolution can occur, Fig. 2. In-line with expectations the magnitude of the catalytic current for hydrogen evolution increases at lower pH values. At high pH (11.5) there is minimal evidence of H$_2$ evolution and the re-oxidation of [Mn^0(bpy(COO)$_2$)(CO)$_3$]$^{3-}$ to reform the dimer occurs at -1.09 V, Fig. 2. Further oxidation to reform the starting complex takes place at -0.30 V. Below pH 4 we find the reduction potential of [Mn^I(bpy(COO)$_2$)(CO)$_3$(OH$_2$)]$^-$ shifts positively (-0.95 V at pH 3.5, Fig. 2) and by pH 2.5, when [Mn^I(bpy(COOH)$_2$)(CO)$_3$(OH$_2$)]$^+$ is expected to be the dominant form, the first reduction is at -0.9 V. Below pH 2.5 accurate determination of the first reduction potential was not possible due to excessive H$_2$ formation at these potentials, even on Hg/Au. The positive shift in reduction potential upon protonation of the carboxylate groups can be rationalized through past

DFT studies which have shown that the first reduction of [Mn(bpy)(CO)$_3$Br] occurs *via* the reduction of the bipyridine ligand and similar behavior would be expected here.[35] In this case protonation of the carboxylic acid groups would stabilize the reduced form of the complex more effectively than the negatively charged carboxylates. Indeed in acetonitrile/water (95:5) under CO$_2$, where protonation of the carboxylate groups may occur (the pK_a of CO$_2$ + H$_2$O in acetonitrile is 23.4),[36] the first reduction is at *ca.* 0.8 V, significantly positive (~0.25 V) of the reduction potential of the deprotonated [Mn^I(bpy(COO)$_2$)(CO)$_3$(CH$_3$CN)]$^-$ under argon in aqueous solution.

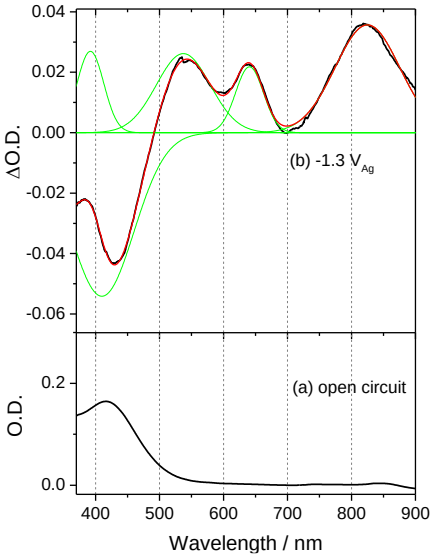

Fig. 3: (a) UV/Vis spectrum of [Mn^I(bpy(COO)$_2$)(CO)$_3$(OH$_2$)]$^-$ at pH 9 (b) UV/Vis difference spectrum following reduction at -1.3V$_{Ag}$ on a carbon foam electrode under an Argon atmosphere K$_2$CO$_3$ (0.5 M) + KCl (0.1 M) at pH = 9. Green lines show the individual Gaussian peaks of the overall multi-peak fit (red line).

An additional reduction between -1.15 and -1.25 V is also observed at pH ≤ 4, Fig. 2. The reductive current increases steeply with decreasing pH (Fig. 5) and at pH 2.5 it reaches 90 μA at -1.21 V (1.8 mA cm^{-2}, Fig. S9) indicating the presence of a catalytic process, likely H_2 evolution, possibly *via* the dimer complex. It is clear that the electrochemistry of $[Mn^{I}(bpy(COOH)_2)(CO)_3(OH_2)]^+$ is significantly more complex than that of $[Mn^{I}(bpy(COO)_2)(CO)_3(OH_2)]^-$ in water and further studies will explore this interesting result. Instead here for the rest of the paper we focus on the electrochemical behavior of $[Mn^{I}(bpy(COO)_2)(CO)_3(OH_2)]^-$ in the presence of CO_2.

At potentials negative of -1.40 V between pH 4-9 under CO_2 we measure a steep increase in current, which exceeds that observed under argon from H_2 evolution, indicating the presence of electrocatalytic CO_2 reduction. At pH 11.5 minimal CO_2 reduction occurs, in-line with past observations in aprotic solvents[37] that a suitably high concentration of Brønsted acid is required to facilitate the protonation of the initially bound CO_2. Finally the complex shows similar behavior to what observed on amalgam electrodes on both glassy carbon (GC) and boron doped diamond (BDD) electrodes (Figs. 4, S10, S11), with a large increase in current under CO_2, indicating that catalysis is not restricted to amalgam electrodes. A plot of current versus pH, from the CVs in Fig. 2, at -1.5 V (Fig. 5) shows that while there is a catalytic CO_2 current at pH 2.5-9, the contribution from proton reduction is minimized at pH 9, while CO_2 reduction is still occurring at an appreciable level, therefore selectivity is expected to be higher under these conditions.

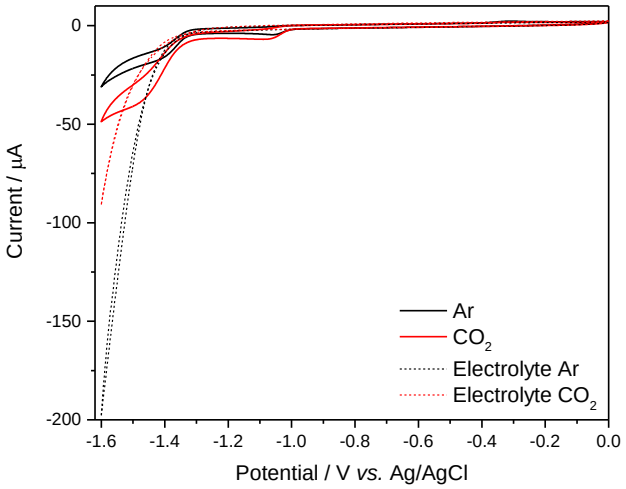

Fig. 4: CV of $[Mn(bpy(COO)_2)(CO)_3(OH_2)]^-$ 0.5 mM at pH 7 (0.1 M KCl, 0.5 M K_2CO_3) recorded at 100 mV s^{-1} on GCE under Ar and CO_2.

Electrolysis experiments carried out at -1.4 V (pH 9) for 22 hours (Fig. S12) confirm that $[Mn^{0}(bpy(COO)_2)(CO)_3]^{3-}$ is an active catalyst for CO_2 reduction in water achieving a bulk TON for CO of 57 (± 13), as measured by gas chromatography of the cell headspace over 3 independent experiments. Significantly a good selectivity for CO_2 reduction to CO in water was achieved with a Faradaic efficiency of 65 (± 15) % for CO production compared to 17 (± 5) % for H_2. Tests for formate by ion chromatography revealed no trace of this product. CVs and UV/Vis spectra recorded post electrolysis showed only slight decomposition of the complex (Fig. S13 and S14) and this coupled to the continued activity over 22 hours indicates reasonable stability.

Control experiments carried out under argon in the presence of the catalyst and the K_2CO_3/$KHCO_3$ electrolyte (pH 9) showed only trace CO, indicating that the source of the carbon is dissolved CO_2 and experiments in the absence of the catalyst showed greatly reduced currents, Fig S15. It is apparent that this complex is one of only a very select group which is able to effectively reduce CO_2 in water.

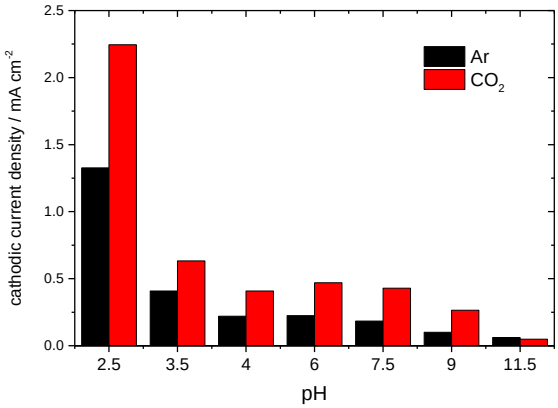

Fig. 5: Current at -1.5 V vs. pH under argon (black) and CO_2 (red) from the CV measurements presented in figure 2.

A small increase in current under CO_2 between -1.05 and -1.40 V with $[Mn^{I}(bpy(COO)_2)(CO)_3(OH_2)]^-$ at pH 9 is also observed. Bulk electrolysis at -1.2 V achieved a TON_{CO} = 10 in 22 hours, a CO:H_2 selectivity of *ca*. 4.5:1, and a total FE of 65 %. -1.20 V is approximately 0.2 V positive of the reduction potential of the dimer complex, suggesting that in water CO_2 reduction may also occur following the oxidative addition of CO_2 and H^+ to a Mn^0 carbonyl dimer in the manner previously described by Bourrez and colleagues.[25] Significantly the observation of CO_2 reduction at -1.2 V corresponds to a very low overpotential, only 0.35 V, similar to that previously reported for a pyrene modified Mn carbonyl complex in water,[28] and amongst the lowest values reported for a water soluble CO_2 reduction electrocatalyst.

CONCLUSION

In conclusion we report a Mn polypyridyl complex for homogeneous electrocatalytic CO_2 reduction in aqueous electrolyte. Solubility is conferred by two carboxylic groups on the polypyridyl ligand and upon dissolution the Mn-Br undergoes ligand exchange to yield the aquo complex. Cyclic voltammetry of the complex shows electrocatalytic CO_2 reduction on both carbon and Hg/Au working electrodes. Bulk electrolysis shows that the catalysts is selective towards CO_2 reduction, achieving a 3.8:1 (CO:H_2) at -1.40 V in aqueous electrolyte. At pH values close to, or below, the pK_a of the carboxylic acid groups very large current increases are observed under argon and CO_2 and new reduction features appear. Future studies will explore the apparent changes in mechanism at low pH.

EXPERIMENTAL SECTION

Milli-Q water (18.2 MΩ) was used throughout. NaOH, KCl, $KHCO_3$, K_2CO_3 and HCl, and were used as received (Fisher Scientific). Na_2CO_3 (anhydrous, Sigma-Aldrich), H_3PO_4 (85 %

wt., Aldrich), H_3BO_3 (> 99.8 %, Merck) and acetic acid (> 99.5 %, Sigma-Aldrich) were used as received. HCl (Fischer, 37 %, analytical reagent grade) was diluted appropriately before use. $[Mn^{I}(bpy)(COOH)_2)(CO)_3Br]$, was synthesized as described previously.[27]

CVs were measured using a Palmsens[3] potentiostat and a pear-shaped flask with a Hg/Au amalgam electrode (geometric surface area = 0.049 cm^2), GC (Glassy carbon) electrode (BASi, geometric surface area = 0.0717 cm^2) or a boron doped diamond (BDD) electrode (Windsor Scientific, geometric surface area = 0.0717 cm^2) as the working electrodes. The amalgam was prepared as follows: a freshly polished gold disc electrode is immersed in mercury for 1-2 minutes, the excess mercury removed and the electrode was left to dry for at least two hours. A Pt coil or mesh were used as the counter electrode and Ag/AgCl (3 M NaCl) was used as the reference electrode (BASi). Experiments were purged with argon, nitrogen or CO_2 for 30 minutes prior to use. The pH was varied by adding HCl or KOH at various concentrations while keeping the purged solution under a blanket of the relevant gas to ensure a common value between Ar/N_2 and CO_2 experiments. Controlled potential electrolysis (CPE) used a Palmsens[3] and a custom mercury pool cell (4.15 cm^2) without stirring or gas bubbling. The counter electrode was separated in a second compartment by a Vycor® frit to minimize re-oxidation of products. The counter electrode compartment contained a 1 M NaOH aqueous solution with 0.1 M ferrocene carboxylic acid as a sacrificial reagent to avoid the formation of Cl_2 or O_2 at the counter electrode. Spectroelectrochemical measurements for the aqueous solutions were carried out in a quartz cuvette using a Palmsens[3] potentiostat, a carbon foam working electrode, platinum mesh counter electrode and Ag/AgCl reference electrode. The Spectrometer beam was centered on the electrode. The potential was held at the indicated values until the resulting current reached a steady state, then a UV-vis spectrum was recorded. Spectroelectrochemical difference spectra were fitted to multiple Gaussian peaks with the peak maxima and peak width of the starting complex fixed at values derived from the fitting of the open-circuit spectrum. SEC in DMF were recorded at 1 mM complex in 0.1 M tetrabutylammonium perchlorate supporting electrolyte using an OTTLE cell (University of Reading, WE, CE = Pt mesh; PRE = Ag wire).

Gas chromatography was performed using an Agilent 6890N employing N6 helium as the carrier gas (5 $ml.min^{-1}$). A 5 Å molecular sieve column (ValcoPLOT, 30 m length, 0.53 mm ID) and a pulsed discharge detector (D-3-I-HP, Valco Vici) were employed. CO peak areas were quantified with multiple calibrant gas injections and were re-calibrated daily. FTIR spectroscopy using a Bruker Vertex spectrometer operating in transmittance mode. UV/Vis absorption data were obtained using a Shimadzu 2550 UV/Vis/NIR spectrophotometer in transmittance mode using either 10 or 2 mm pathlength quartz cuvette.

High-resolution mass spectra (HRMS) for verification of elemental composition were recorded on a Bruker Compact mass spectrometer. The system has a mass resolution of 30,000 (FSW @ 1222 m/z) and mass accuracy better than 1-2 ppm RMS error (depending on calibration mode). Agilent Tune Mix- L was used for calibration, control software: otofControl 4.1 and Data Analysis 4.4. Samples were infused via syringe pump at a rate of 150 µl/hr. ESI +/- experiments were recorded over the range 50-2000 m/z, end-plate offset 500V capillary 4500V, nebulizer 2.0 bar, dry gas 8.0 L/min, and dry temperature 180°C.

Variable pH UV/Vis spectra were recorded using Britton-Robinson buffers of various starting pH values.[38] pH values were measured using a VWR SympHony SP70P pH meter, which was calibrated before each use using pH 4, 7 and 10 standards. Concentration-dependent UV/Vis spectra were recorded as follows: accurately weighed solutions of complex were made up in a series of volumetric flasks covered in aluminum foil. Each flask was sonicated for 10 minutes to ensure complete dissolution of the complex or saturation of the solution had occurred. Aliquots of each solution were centrifuged at 10000 rpm for 5 minutes and the UV/Vis spectra of the supernatant measured.

ASSOCIATED CONTENT

Supporting Information

UV/Vis and FTIR spectroscopies, mass spectrometry, further cyclic voltammetry, bulk electrolysis data.

Raw experimental data for all figures is freely available from the University of Liverpool Research Data Catalogue at DOI: 10.17638/datacat.liverpool.ac.uk/497

AUTHOR INFORMATION

Corresponding Author* acowan@liverpool.ac.uk.

† These authors contributed equally to this work.

The authors declare no competing financial interests

ACKNOWLEDGEMENT

This work was funded by the EPSRC (EP/K006851/1, EP/N010531/1). CLS thanks the University of Liverpool for a DTA studentship. SFI is acknowledged for Grant No. 15/SIRG/3517 (JJW). HRMS were acquired at the Mass Spectrometry Unit, Trinity College Dublin.

REFERENCES

1. Inglis, J. L., MacLean, B. J., Pryce, M. T. & Vos, J. G. Electrocatalytic pathways towards sustainable fuel production from water and CO2. *Coord. Chem. Rev.* **256,** 2571–2600 (2012).
2. Tu, W., Zhou, Y. & Zou, Z. Photocatalytic Conversion of CO2 into Renewable Hydrocarbon Fuels: State-of-the-Art Accomplishment, Challenges, and Prospects. *Adv. Mater.* **26,** 4607–4626 (2014).
3. Cowan, A. J. & Durrant, J. R. Long-lived charge separated states in nanostructured semiconductor photoelectrodes for the production of solar fuels. *Chem. Soc. Rev.* **42,** 2281–2293 (2013).
4. White, J. L. *et al.* Light-Driven Heterogeneous Reduction of Carbon Dioxide: Photocatalysts and Photoelectrodes. *Chem. Rev.* **115,** 12888–12935 (2015).
5. Costentin, C., Robert, M., Savéant, J.-M. & Tatin, A. Efficient and selective molecular catalyst for the CO 2 -to-CO electrochemical conversion in water. *Proc. Natl. Acad. Sci.* **112,** 6882–6886 (2015).
6. Beley, M., Collin, J.-P., Ruppert, R. & Sauvage, J.-P. Nickel(II)-cyclam: an extremely selective electrocatalyst for reduction of CO2 in water. *J. Chem. Soc. Chem. Commun.* **2,** 1315–1316 (1984).
7. Beley, M., Collin, J. P., Ruppert, R. & Sauvage, J. P. Electrocatalytic reduction of carbon dioxide by nickel cyclam2+ in water: study of the factors affecting the efficiency and the selectivity of the process. *J. Am. Chem. Soc.* **108,** 7461–7467 (1986).
8. Schneider, J. *et al.* Nickel(ii) macrocycles: highly efficient electrocatalysts for the selective reduction of CO2 to CO. *Energy Environ. Sci.* **5,** 9502 (2012).
9. Neri, G. *et al.* A functionalised nickel cyclam catalyst for CO 2 reduction: electrocatalysis, semiconductor surface immobilisation and light-driven electron transfer. *Phys. Chem.*

Chem. Phys. **17,** 1562–1566 (2015).
10. Neri, G. *et al*. Photochemical CO $_2$ reduction in water using a co-immobilised nickel catalyst and a visible light sensitiser. *Chem. Commun.* **52,** 14200–14203 (2016).
11. Neri, G., Aldous, I. M., Walsh, J. J., Hardwick, L. J. & Cowan, A. J. A highly active nickel electrocatalyst shows excellent selectivity for CO2 reduction in acidic media. **7,** 1521–1526 (2016).
12. Kang, P., Meyer, T. J. & Brookhart, M. Selective electrocatalytic reduction of carbon dioxide to formate by a water-soluble iridium pincer catalyst. *Chem. Sci.* **4,** 3497 (2013).
13. Nakada, A. & Ishitani, O. Selective Electrocatalysis of a Water-Soluble Rhenium(I) Complex for CO2Reduction Using Water As an Electron Donor. *ACS Catal.* **8,** 354–363 (2018).
14. Bourrez, M., Molton, F., Chardon-Noblat, S. & Deronzier, A. [Mn(bipyridyl)(CO)3Br]: an abundant metal carbonyl complex as efficient electrocatalyst for CO2 reduction. *Angew. Chem. Int. Ed. Engl.* **50,** 9903–9906 (2011).
15. Agarwal, J. *et al.* NHC-Containing Manganese(I) Electrocatalysts for the Two-Electron Reduction of CO2. *Angew. Chem. Int. Ed. Engl.* **53,** 5152–5155 (2014).
16. Agarwal, J. *et al.* Exploring the effect of axial ligand substitution (X = Br, NCS, CN) on the photodecomposition and electrochemical activity of [MnX(N–C)(CO) $_3$] complexes. *Dalt. Trans.* **44,** 2122–2131 (2015).
17. Machan, C. W. *et al.* Electrocatalytic Reduction of Carbon Dioxide by Mn(CN)(2,2′-bipyridine)(CO) $_3$: CN Coordination Alters Mechanism. *Inorg. Chem.* **54,** 8849–8856 (2015).
18. Franco, F. *et al.* A local proton source in a [Mn(bpy-R)(CO) $_3$ Br]-type redox catalyst enables CO $_2$ reduction even in the absence of Brønsted acids. *Chem. Commun.* **50,** 14670–14673 (2014).
19. Stor, G. J., Morrison, S. L., Stufkens, D. J. & Oskam, A. The Remarkable Photochemistry of fac-XMn(CO)3(α-diimine) (X = Halide): Formation of Mn2(CO)6(α-diimine)2 via the mer Isomer and Photocatalytic Substitution of X− in the Presence of PR3. *Organometallics* **13,** 2641–2650 (1994).
20. Stanbury, M., Compain, J.-D. & Chardon-Noblat, S. Electro and photoreduction of CO 2 driven by manganese-carbonyl molecular catalysts. *Coord. Chem. Rev.* **361,** 120–137 (2018).
21. Hartl, F., Rossenaar, B. D., Stor, G. J. & Stufkens, D. J. Role of an electron-transfer chain reaction in the unusual photochemical formation of five-coordinated anions Mn(CO)(3)(alpha-diimine)(-) from fac- Mn(X)(CO)(3)(alpha-diimine) (X=halide) at low temperatures. *Recl. Trav. Chim. Pays-Bas* **114,** 565- (1995).
22. Machan, C. W., Sampson, M. D., Chabolla, S. A., Dang, T. & Kubiak, C. P. Developing a Mechanistic Understanding of Molecular Electrocatalysts for CO2 Reduction using Infrared Spectroelectrochemistry. *Organometallics* **Accepted A,** Ahead of Print (2014).
23. Hartl, F., Rosa, P., Ricard, L., Le Floch, P. & Záliš, S. Electronic transitions and bonding properties in a series of five-coordinate '16-electron' complexes [Mn(CO)3(L2)]-(L2= chelating redox-active π-donor ligand). *Coordination Chemistry Reviews* **251,** 557–576 (2007).
24. Smieja, J. M. *et al*. Manganese as a substitute for rhenium in CO2 reduction catalysts: the importance of acids. *Inorg. Chem.* **52,** 2484–2491 (2013).
25. Bourrez, M. *et al.* Pulsed-EPR evidence of a manganese(II) hydroxycarbonyl intermediate in the electrocatalytic reduction of carbon dioxide by a manganese bipyridyl derivative. *Angew. Chem. Int. Ed. Engl.* **53,** 240–243 (2014).
26. Walsh, J. J., Neri, G., Smith, C. L. & Cowan, A. J. Electrocatalytic CO 2 reduction with a membrane solution †. *Chem. Commun.* **50,** 12698–12701 (2014).
27. Walsh, J. J. *et al*. Improving the efficiency of electrochemical CO $_2$ reduction using immobilized manganese complexes. *Faraday Discuss.* **183,** 147–160 (2015).
28. Reuillard, B. *et al.* Tuning Product Selectivity for Aqueous CO 2 Reduction with a Mn(bipyridine)-pyrene Catalyst Immobilized on a Carbon Nanotube Electrode. *J. Am. Chem. Soc.* **139,** 14425–14435 (2017).
29. Sato, S., Saita, K., Sekizawa, K., Maeda, S. & Morikawa, T. Low-energy electrocatalytic CO2 reduction in water over Mn-complex catalyst electrode aided by a nanocarbon support and K+ cations. *ACS Catal.* **8,** 4452−4458 (2018).
30. Nazeeruddin, M. K. & Kalyanasundaram, K. Acid-Base Behavior in the Ground and Excited States of Ruthenium(II) Complexes Containing Tetraimines or Dicarboxybipyridines as Protonatable Ligands. *Inorg. Chem.* **28,** 4251–4259 (1989).
31. Zheng, G. Y., Wang, Y. & Rillema, D. P. Acid - Base Properties of the Ground and Excited States of Ruthenium (II). *Inorg. Chem.* **35,** 7118–7123 (1996).
32. Watanabe, T. *et al.* Giant electric double-layer capacitance of heavily boron-doped diamond electrode. *Diam. Relat. Mater.* **19,** 772–777 (2010).
33. Walsh, J. J. *et al*. Directing the mechanism of CO2 reduction by a Mn catalyst through surface immobilization. *Phys. Chem. Chem. Phys.* **20,** 6811–6816 (2018).
34. Hans, K., Haar, D., Stufkens, D. J. & Oskam, A. Metal to ligand charge-transfer photochemistry of metal-metal-bonded complexes. 7. Photochemistry of (CO)4CoM(CO)3(bpy) (M = Mn, Re; bpy = 2,2'-bipyridine): Photocatalytic Disproportionation of the Manganese Complex in the Presence of PR3. *Inorg. Chem.* 75–81 (1989).
35. Riplinger, C. & Carter, E. A. Influence of Weak Brønsted Acids on Electrocatalytic CO $_2$ Reduction by Manganese and Rhenium Bipyridine Catalysts. *ACS Catal.* **5,** 900–908 (2015).
36. Grills, D. C. *et al.* Electrocatalytic CO2 Reduction with a Homogeneous Catalyst in Ionic Liquid: High Catalytic Activity at Low Overpotential. *J. Phys. Chem. Lett.* **5,** 2033–2038 (2014).
37. Riplinger, C., Sampson, M. D., Ritzmann, A. M., Kubiak, C. P. & Carter, E. A. Mechanistic Contrasts between Manganese and Rhenium Bipyridine Electrocatalysts for the Reduction of Carbon Dioxide. *J. Am. Chem. Soc.* **136,** 16285–16298 (2014).
38. Mongay, C. & Cerda, V. A Britton-Robinson buffer of known ionic strength. *Ann. Chim.* **64,** 409–412 (1974).

TOC GRAPHIC

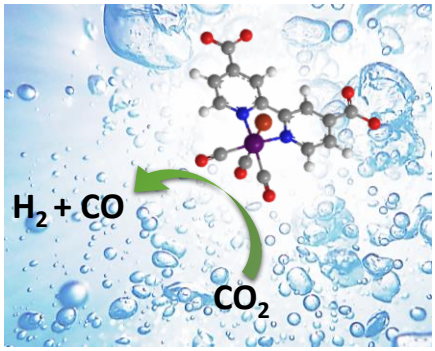
$H_2 + CO$
CO_2